Plant, Cell & Environment

Plant, Cell and Environment (2013) doi: 10.1111/pce.12225

Original Article

The dynamic pipeline: hydraulic capacitance and xylem hydraulic safety in four tall conifer species

Katherine A. McCulloh[1]*, Daniel M. Johnson[2], Frederick C. Meinzer[3] & David R. Woodruff[3]

[1]Department of Forest Ecosystems and Society, Oregon State University, Corvallis, OR 97331, USA, [2]Nicholas School of the Environment, Duke University, Box 90328, Durham, NC 27708, USA and [3]Pacific Northwest Research Station, USDA Forest Service, Corvallis, OR 97331, USA

ABSTRACT

Recent work has suggested that plants differ in their relative reliance on structural avoidance of embolism versus maintenance of the xylem water column through dynamic traits such as capacitance, but we still know little about how and why species differ along this continuum. It is even less clear how or if different parts of a plant vary along this spectrum. Here we examined how traits such as hydraulic conductivity or conductance, xylem vulnerability curves, and capacitance differ in trunks, large- and small-diameter branches, and foliated shoots of four species of co-occurring conifers. We found striking similarities among species in most traits, but large differences among plant parts. Vulnerability to embolism was high in shoots, low in small- and large-diameter branches, and high again in the trunks. Safety margins, defined as the pressure causing 50% loss of hydraulic conductivity or conductance minus the midday water potential, were large in small-diameter branches, small in trunks and negative in shoots. Sapwood capacitance increased with stem diameter, and was correlated with stem vulnerability, wood density and latewood proportion. Capacitive release of water is a dynamic aspect of plant hydraulics that is integral to maintenance of long-distance water transport.

Key-words: capacitance; conifers; hydraulic conductance; safety margins; vulnerability curves.

INTRODUCTION

Water movement in plants occurs along a gradient of decreasing water potential from roots to leaves. Thus, while transpiring, the leaves of all plants experience more negative water potentials than their roots. Although all plants experience the decline in water potential distally, it is compounded in tall trees because of the hydrostatic gradient and path length associated with their stature. This gradient imposes an additional drop in the pressure potential of the xylem that is associated with raising water to great heights, and the xylem pressure declines by 0.01 MPa m^{-1} in addition to the drop required to overcome frictional resistance along the hydraulic pathway. Whether or not the water potentials experienced by the distal organs are inherently more stressful depends on the vulnerability of those tissues to loss of function because of the water stress, such as drought-induced loss of hydraulic conductivity, as well as the ability of leaves to accumulate enough solutes to maintain turgor and sustain the necessary driving force to draw water from the soil.

We often compare the sensitivity of plant organs to drought through the use of vulnerability curves, which indicate the loss of hydraulic conductivity or conductance in a plant organ as water potentials decline. A commonly used metric to compare vulnerability curves is the P_{50}, which is the pressure at which 50% of the hydraulic conductivity or conductance has been lost. The P_{50} is a useful metric because of its location on the steepest part of the vulnerability curve, which means that even a slight drop in pressure would result in a large increase in the percent loss of hydraulic conductivity and the risk of runaway embolism is large (Tyree & Sperry 1988). Plants exhibit an impressive range of vulnerability and P_{50}s, even within a given habitat (Pockman & Sperry 2000; Maherali *et al*. 2004; Blackman *et al*. 2012). Even within a plant, the difference between organs can be large (e.g. Domec *et al*. 2006; Maherali *et al*. 2006; Willson *et al*. 2008). Vulnerability to drought-induced embolism can increase or decrease from branches to leaves (e.g. Hao *et al*. 2008; Chen *et al*. 2009). In conifers, although, it seems that leaves tend to be much more vulnerable than stems (Johnson *et al*. 2011).

A more informative measure to compare species than simply using the P_{50}, which does not reflect the inherent risk to the system because of differences in operating pressures, is to compare safety margins (Pockman & Sperry 2000; Brodribb *et al*. 2003; Brodribb & Holbrook 2004; Pratt *et al*. 2007b; Meinzer *et al*. 2009; Bucci *et al*. 2012; Choat *et al*. 2012; Johnson *et al*. 2012), such as the difference between the midday water potential of an organ and the P_{50}. This value is much more informative because it indicates how close to the P_{50} an organ operates. As with P_{50}s, there are a wide range of safety margins exhibited by plants (Meinzer *et al*. 2009; Choat *et al*. 2012). Small-diameter stems have been studied most extensively, and conifers appear to have larger safety margins than some angiosperms, although many angiosperms (particularly those in Mediterranean and cold desert environments) also have large values (Martínez-Vilalta

Correspondence: K. McCulloh. E-mail: kmcculloh@wisc.edu

*Present address: Department of Botany, University of Wisconsin-Madison, Madison, WI 53706, USA.

et al. 2002; Vilagrosa *et al*. 2003; Pratt *et al*. 2007a; Bucci *et al*. 2013).

Although much less is known about general patterns in leaf hydraulics across species, there also appears to be a wide range of safety margins in that organ. Leaves of angiosperm species seem to span the range from small (or even negative, i.e. the midday water potential is more negative than the P_{50}) to large safety margins (Johnson *et al*. 2009, 2011; Zufferey *et al*. 2011; Bucci *et al*. 2013). Conifers, particularly those in the Pinaceae, exhibit negative safety margins, and diurnal measurements indicate that the leaves of some conifers undergo cycles of loss and recovery of hydraulic conductance on daily bases (Woodruff *et al*. 2007; Johnson *et al*. 2009, 2011).

Because of the difficulty of measuring samples from larger-diameter branches and bole wood of mature trees, less research has been conducted on these sample types and so even less is known about their vulnerability to embolism. Most work on bole wood has been done on conifer species (e.g. Domec & Gartner 2001; Rosner *et al*. 2006; Dunham *et al*. 2007), although Choat *et al*. (2005) did find that individual vessels in the trunks of mature *Acer saccharum* were more resistant to embolism than those in 1-year-old stems. However, this result may have been due to the presence of primary xylem in the young stems, because no differences were found in the embolism resistance of vessels in other stem age classes compared with the trunk. Interestingly, when trunks and smaller-diameter stems within conifers are compared, the pattern has been the reverse: smaller-diameter stems are more resistant to embolism (Domec *et al*. 2006; Dunham *et al*. 2007). Safety margins are extremely difficult to estimate in large diameter organs because of the lack of inexpensive, instantaneous methods for estimating operating pressures.

Whether we compare the same organ among species, or different organs within a species, there appears to be a continuum of strategies to cope with water stress. At one end of the continuum are species and organs that rely on structural features to avoid embolism formation. These tissues tend to have more negative P_{50} values and larger safety margins. Attaining more negative P_{50} values requires thicker conduit walls (Hacke *et al*. 2001; Pittermann *et al*. 2006) and changes in the dimensions of the interconduit pits (Domec *et al*. 2006, 2008; Choat *et al*. 2007). At the other end are tissues that maintain milder operating pressures through reliance on capacitance and stringent stomatal control. These organs tend to have less negative P_{50}s and smaller safety margins. Capacitance is a measure of a tissue's ability to store water, and buffers the system by both reducing the magnitude of the xylem pressure drop caused by increases in transpiration (over the range of pressures of capacitive discharge) and by slowing the xylem pressure drop, which may provide sufficient time for stomata to react. The milder operating pressures that these tissues experience allow for thinner conduit walls, which results in wood that is less dense and has a greater volume fraction that could be devoted to capacitive storage.

Along this continuum there appears to be a change in the reliance on refilling of embolized conduits. Species or organs that have less negative P_{50} values may be better at refilling emboli after periods of water stress than those with more negative values. In an experiment in which saplings from seven angiosperm species were stressed to their P_{50}, Ogasa *et al*. (2013) found that species with less negative P_{50} values had lower wood density and were better able to recover from the imposed drought. Species or organs with high wood density and low P_{50} values may lack the volume of the living cells required to refill conduits efficiently (Zwieniecki & Holbrook 2009; Nardini *et al*. 2011; Johnson *et al*. 2012). These results suggest there may be a tradeoff between embolism resistance and the ability to repair embolism across species and across different organs in the same species (e.g. leaves and stems). However, Urli *et al*. (2013) observed the opposite pattern. They found that more drought-resistant species (i.e. those with lower P_{50}s) were better able to recover from considerable loss of conductivity and that the point at which recovery was no longer possible was well described by the P_{88} (i.e. the pressure causing an 88% reduction in hydraulic conductivity). It is clear that we do not fully understand the limitations of refilling across species.

Water movement through plants requires the coordinated transport by all organs, but studies on mature trees often ignore everything except leaves, small-diameter branches and small-diameter roots. Very little is known about how various parameters of a plant's hydraulic architecture change from trunk to twig in large trees. Although we do have a good understanding of xylem anatomical changes along this path, such as vessel diameters decreasing and vessel frequency increasing (e.g. Zimmermann 1978; Dunham *et al*. 2007), our knowledge of the functional consequences of these structural changes is less well described.

In the Pacific Northwest region of North America, the combination of dry, sunny summers, wet winters and relatively mild temperatures allow the growth of the world's tallest trees. At the site where this research was conducted, the Wind River Field Station (formerly the Wind River Canopy Crane Research Facility) in Southern Washington, the oldest trees are approximately 500 years old and the tallest trees are 60–65 m tall (Shaw *et al*. 2004). The forest is dominated by Douglas-fir (*Psuedotsuga menziesii*) and western hemlock (*Tsuga heterophylla*), and has lower densities of tall western redcedar (*Thuja plicata*) and grand fir (*Abies grandis*). Here, we compare the anatomy, explore differences in functional traits such as vulnerability to embolism, capacitance and hydraulic conductivity in these species. These traits are examined in samples taken from their trunks, large-diameter branches, small-diameter branches and shoots, which we will refer to as separate 'organs.' We asked two main questions in this study. First, do these co-occurring species differ in their reliance on static (i.e. structural features) versus dynamic (i.e. capacitance) means for maintaining the integrity of their water transport networks during normal, daily cycles of water stress? Second, are there changes in the relative reliance on these static versus dynamic mechanisms in different organs along an axial gradient from trunk to twig?

MATERIALS AND METHODS

Plant material collection

Samples were taken during the summers of 2009 and 2010 from conifers growing in an old-growth Douglas-fir and western hemlock forest in southern Washington at the Wind River Field Station (45°49′ 13.76″ N, 121°57′ 06.88″ W). During the time of this study, this facility had a 75-m tall canopy crane with an 85-m long jib to which a gondola was attached that provided access to the crowns of the trees. The four species examined here represent the main overstory conifer species at the site. Those species are grand fir [*Abies grandis* (Dougl.) Forbes], Douglas-fir [*Pseudotsuga menziesii* (Mirbel) Franco.], western redcedar [*Thuja plicata* Donn.] and western hemlock [*Tsuga heterophylla* (Raf.) Sarg.]. Branches were collected from the tops of four to seven representatives using the crane gondola. Cores were taken from the trunk using a 12.5- or 5.0-mm borer (depending on measurements, see later) at ~1.3 m above the ground from at least two individuals from each species. Branches and cores were wrapped in wet paper towels and placed in sealable plastic bags after collection. Bags were stored in a cooler for transport back to the laboratory at Oregon State University the same day.

Shoot hydraulic measurements

The vulnerability of terminal, leaf-bearing shoots (approximately 2–3 cm long) to loss of hydraulic conductance with declining water potential (i.e. vulnerability curves) was measured in three species. Vulnerability curves for shoots of Douglas-fir had been made from the tops of trees at the site for a previous study (Woodruff *et al*. 2007) and parameters from these curves were used for comparison here. The hydraulic conductance of shoots (K_{SH}) was measured using the timed rehydration kinetics method (Brodribb & Holbrook 2003). This method requires two shoots with the same water potential. The water potential of one shoot is measured. Then, after partially rehydrating the second shoot for a given amount of time (t), its water potential is measured. K_{SH} was calculated as:

$$K_{SH} = C \ln(\Psi_i/\Psi_f)/t \quad (1)$$

where C is shoot capacitance, Ψ_i and Ψ_f leaf water potential before and immediately after partial rehydration, respectively. The time for rehydration varied from approximately 30–90 s, depending on the value of Ψ_i. Samples with more negative Ψ_i values were allowed a longer rehydration time. Vulnerability curves were constructed on shoots from branch samples ~0.5 m long that were collected early in the morning to minimize water stress. After transport to the laboratory, branches were re-cut under water and allowed to rehydrate in distilled water for 4–5 h so that all shoots had water potentials between 0 and –0.1 MPa. After rehydration, branches were dried on the lab bench to various water potentials, and were then placed in plastic bags in the dark to allow water potentials to equilibrate. Paired shoots of similar size were used for each K_{SH} measurement.

Values of C were calculated from pressure-volume curves (Tyree & Hammel 1972) made on three to five shoots. These curves are made by alternately measuring shoot mass and water potential as the shoots dehydrated. The leaf water potential at the turgor loss point is the inflection point on a graph of the inverse of the water potential versus relative water content (RWC). C values were calculated before and after the turgor loss point as the slope of relationship between leaf water potential and RWC. If Ψ_i and Ψ_f spanned the turgor loss point, we used the average pre- and post-turgor loss point capacitance value to calculate K_{SH}.

Stem hydraulic measurements

Stems of small and large diameters (Table 1) were used for measurements of hydraulic conductivity and vulnerability to drought-induced embolism. The term 'large' is used to distinguish this size class from the small-diameter stems. The large stems were ~1 cm in diameter and were approximately twice as wide as the small-diameter stems. The cut ends of all stem samples were re-cut underwater with fresh razor blades. Cut segments were submerged in a filtered perfusion solution of water mixed with a small amount of concentrated hydrochloric acid, which reduced the pH to two and retarded microbial growth. A partial vacuum was applied overnight to the solution and stems to refill all embolized tracheids with water. Before measurements began and with the stems still under partial vacuum, the cut ends of all segments were inspected to ensure no bubbles were still being pulled from the xylem.

The morning after segments were flushed, hydraulic conductivity measurements were begun to construct vulnerability curves, which are created from alternately measuring hydraulic conductivity and radially injecting air at

Table 1. Species collection heights, branch and trunk diameters, and tracheid diameters for small and large diameter branches and trunks

Species	Collection height (m)	Mean diameter (cm) – small	Mean diameter (cm) – large	Mean diameter (cm) – trunk	Tracheid diameter – small (μm)	Tracheid diameter – large (μm)	Tracheid diameter – trunk (μm)
Abies grandis	50.4 (1.5)	0.47 (0.04)	0.93 (0.05)	68.8 (12.6)	9.5 (0.5)	14.8 (1.0)	33.9 (4.8)
Pseudotsuga menziesii	59.8 (2.3)	0.52 (0.08)	1.06 (0.09)	135.2 (12.6)	11.2 (0.3)	14.1 (0.6)	25.3 (5.2)
Thuja plicata	51.8 (1.2)	0.61 (0.07)	0.97 (0.08)	107.9 (6.2)	10.1 (0.6)	13.2 (2.2)	33.7 (5.4)
Tsuga heterophylla	54.5 (0.5)	0.59 (0.05)	0.92 (0.08)	87.5 (1.8)	11.4 (0.5)	14.3 (0.1)	31.6 (3.6)

Numbers in parentheses indicate standard errors. Tracheid diameters were measured on branches or cores used for vulnerability curves.

known, high pressures. The 'air-injection' method (Sperry & Saliendra 1994) assumes that air seeds between tracheids at a pressure that has the same magnitude, but opposite sign (i.e. positive versus negative), as *in situ*. Hydraulic conductivity was measured by timing the intervals for water to reach successive gradations on a pipette attached with tubing to the distal end of the segment, and dividing this volume flow rate by the pressure gradient used to induce flow across the sample. The pressure gradient was created by a hydrostatic pressure head, which was usually approximately 80 cm high. Air pressures imposed on stems between each measurement of k_h were increased in 1.0 MPa increments. Vulnerability curves were graphed by comparing the percent loss in k_h relative to the maximum versus the applied pressure. Xylem-area specific conductivity (k_s) was determined by dividing maximum k_h by the xylem cross-sectional area of the branch.

Maximum k_h was measured on 12.5 mm cores taken from the trunks of the trees. To make these measurements, the cores were cut under water with a razor blade into ~10-mm long axially oriented segments that were ~3 mm in diameter. Care was taken to ensure the axial tracheids ran lengthwise in the segment, and this was confirmed by making cross sections of the segments after hydraulic measurements were complete (Supporting Information Fig. S1). After flushing the segments overnight in pH 2 water as described earlier, the segments were fitted to tubing and k_h was measured gravimetrically. To determine the xylem cross-sectional area for calculating k_s, the fresh volume of each segment, which was determined by the displacement of water on a scale, was divided by the length (this process was necessary, because the segments were not entirely round, but instead were polygons in cross section).

Vulnerability curves of 12.5-mm cores from the base of trunks were made using ultrasonic acoustic emissions. Sections of the xylem were cut from cores ~5 mm from the cambium that were ~3-mm thick (radially). The circular segment was then cut in half and, after overnight vacuum infiltration in water, the flat surface was placed against the surface of the acoustic sensor (R15α; Physical Acoustics Corp., Princeton Junction, NJ, USA). The sensor and wood segment were clamped together to maximize contact between them. After weighing the clamp, sensor and wood piece, the sensor was attached to a datalogger (Pocket AE; Physical Acoustic Corp.) to record acoustic emissions from the wood. Periodically (roughly every half hour), data logging was paused, and the clamp–sensor–wood complex was weighed. Samples air-dried for 4–7 h. Datalogging was stopped after no acoustic emissions were detected for 10–20 min. Wood samples were dried in a drying oven at 100 °C for three days to determine dry mass, and RWC was calculated for each repeated measurement as

$$RWC = \frac{M_f - M_d}{M_s - M_d} \quad (2)$$

where M_f is the sample mass for the measurement, M_d is the dry mass and M_s is the saturated mass of the sample. From the water release curves described below, RWC values were converted to water potentials, and vulnerability curves were developed. The acoustic emissions method has been verified by comparing with other methods of determining vulnerability curves, which directly measure loss of hydraulic conductivity, in conifers, including Douglas-fir, in a number of studies (Cochard 1992; Rosner *et al*. 2006, 2008, 2009; Barnard *et al*. 2011; Mayr & Rosner 2011).

Water potential measurements and estimates

Water potentials were measured on shoots from all four species and were published in previous work (McCulloh *et al*. 2011). Three shoots were measured at the tops of three individuals from each species before sunrise and at midday (1100–1300 h). After measuring the predawn water potentials on each individual, we placed plastic bags covered in aluminium foil over branches. During the visit to each tree at midday, we measured the water potential of shoots from within the bags and used these values as estimates of branch water potential (Begg & Turner 1970).

Trunk water potentials were estimated from the Darcy's law relationship, which indicates $\Delta P\, l^{-1} = J_s/k_s$, where $\Delta P\, l^{-1}$ is the tension gradient (MPa m^{-1}), J_s is the sap flux density (g m^{-2} s^{-1}) and k_s is the specific conductivity (kg MPa^{-1} m^{-1} s^{-1}), which was measured as described earlier. Maximum sap flux rates on clear days during the growing season were measured with heat dissipation probes (James *et al*. 2002) inserted to a depth of 2 cm in the boles of one *Pseudotsuga*, two *Thuja* and three *Tsuga* individuals. During the period of maximum sap flux, water potential values would have reached their daily minima and conditions were assumed to be nearly steady-state with minimum influence of capacitance. Soil water potentials were estimated by correcting the predawn water potentials made on shoots for the heights from which they were collected using the hydrostatic gradient. Using the calculated tension gradients and the soil water potentials, trunk water potentials were estimated using Darcy's law assuming that the length was 2 m (i.e. $\Psi_{trunk} = \Psi_{soil} - \Delta P/l \times 2$) for each species. Although the length of 2 m is less than the distance the water would travel from the roots to the trunk, the tension gradient within the roots is expected to be lower than within the trunk because of the larger diameter tracheids there (Dunham *et al*. 2007). To determine the effect of path length on the predicted loss of hydraulic conductivity, we also estimated the tension using a length of 10 m, which resulted in a 0.5, 0.9 and 3.8% increase in the predicted percent loss of conductivity at midday over the tensions predicted using 2 m in *Pseudotsuga*, *Thuja* and *Tsuga*, respectively. The Ψ_{soil} was calculated by correcting the predawn water potentials for the height of the foliage using the hydrostatic gradient (0.01 MPa m^{-1}).

Wood capacitance measurements

Small chunks of small and large diameter branches (~1 cm axially) and 5 mm cores (~1 cm radially) from each species were used to construct moisture release curves. Three to five samples were made per species for the small and large branches, and four to six bole wood core samples were made

per species. Two (for *Abies*) or four (all other species) individuals were sampled. For the cores, the segment used began approximately 5 mm inside of the cambium. All samples were vacuum-infiltrated overnight in water. The saturated samples were then blotted on a paper towel to remove excess water, weighed and placed in screen cage thermocouple psychrometer chambers (83 series; JRD Merrill Specialty Equipment, Logan, UT, USA). These chambers were then triple-bagged and submerged in a cooler of water for 2–3 h to allow the sample to equilibrate with the chamber air. After the equilibration period, the millivolt readings were recorded using a psychrometer reader (either an 85 series; JRD Merrill Specialty Equipment or a Psypro; Wescor, Logan, UT, USA). Following the measurement, the samples were removed from the chambers, weighed and allowed to dry on the laboratory bench for approximately half an hour before repeating the process (except for the saturation step). The mV output by the psychrometer was converted to MPa based on calibration curves from salt solutions of known water potentials. Samples were measured repeatedly until water potential values reached ~ –4 MPa. Samples were then placed in the drying oven for at least three days before weighing the dry mass. For each of the repeated measurements, the RWC was calculated. From RWC, relative water deficit (RWD) was calculated as 1 – RWC. The product of RWD and the mass of water per unit tissue volume at saturation (M_w) yielded the cumulative mass of the water lost at each measurement on a volumetric basis. M_w was calculated as:

$$M_w = \left(\frac{M_s}{M_d} \times \rho\right) - \rho \quad (3)$$

where ρ is wood density. Then by graphing moisture release curves, which compare the cumulative mass of water lost versus the sapwood water potential, the capacitance of the sample could be estimated by plotting a regression to the initial, nearly linear, phase of the plot, which encompassed the likely *in situ* physiological operating range of stem water potential (Meinzer *et al*. 2003, 2008). The starting point of this regression was 0, because it is physically impossible for water to be released at 0 MPa. The end point of the regression used to calculate capacitance from the moisture release curves was determined in a manner similar to the analyses of pressure-volume curves in leaves. To determine this end point, the data were plotted as $-1/\Psi$ versus water released. A linear regression was developed from the linear portion of this plot (i.e. high water released values) and points were added until the coefficient of variation began to decline. The final data point before the decline in the coefficient of variation was determined to be the inflection point on the moisture release curve. Capacitance was calculated as the slope of the regression between 0 and the inflection point on the plot of Ψ versus water released.

Wood morphological and anatomical measurements

Wood density was measured for all stem segments used for hydraulics and for one core from each of two trees per species. For the cores, the segment was similarly located to those which were used to estimate capacitance (i.e. approximately 1 cm radially, which was taken approximately 0.5 cm inside of the cambium). For the branches, bark was removed. To calculate wood density, saturated samples were submerged in a cup of water on a scale. The change in mass caused by the sample is equal to the volume of water displaced, and the mass was converted to volume by dividing by the density of water at standard temperature and pressure (1 g cm^{-3}). After submersion, samples were dried in an oven at 70 C overnight and the dry mass measured. Wood density was calculated as the oven-dry mass per fresh volume.

Tracheid diameters and latewood fraction were measured on a subset of samples used for vulnerability curve measurements. Cross sections were made of these wood segments using a sliding microtome. The sections were mounted in glycerine and images of them were taken using a Photometrics Coolsnap camera (Tucson, AZ, USA) mounted on a Nikon Eclipse E400 microscope connected to a PC using Metavue software (Universal Imaging Corp., Downington, PA, USA). Images were analyzed using the freeware software ImageJ (NIH, USA, http://rsb.info.nih.gov/ij/). Tracheids in one to two adjacent rows were measured from cambium to pith (for branches) or for ~3–4 years (for trunks). This resulted in at least 100 tracheids measured. The area of the lumen was measured, and the lumen diameter was calculated by assuming the area was the shape of a circle. Latewood fraction was measured by measuring the length (radially) of the entire growth ring and only the latewood portion, and then calculating the ratio of latewood length: total growth ring length.

Data analysis

Sigma plot version 11 (Systat Software, Inc., Chicago, IL, USA) was used to create curves for all vulnerability curves and water release curves. Vulnerability curves were fit to data with three-parameter sigmoid functions. The values of P_{50} and P_{12} for each species and organ were determined to be different when 95% confidence intervals did not overlap. Water release curves were fit to data with three-parameter Gompertz functions. Relationships of the linear portions of the water release curves, which indicate capacitance, were estimated using the standard major axis (SMA) line-fitting method. The slopes were calculated and compared within species in SMATR freeware (Warton *et al*. 2006; http://www.bio.mq.edu.au/ecology/SMATR/).

RESULTS

Vulnerability curves made on needle-bearing shoots (hereafter shoots), small- and large-diameter branches, and trunks indicated a great deal of variation across these ranks within species. Among the four species, though, the trends of vulnerability with rank were very similar. Generally, the shoots of all species were extremely vulnerable (Fig. 1) both relative to the midday water potentials they normally experienced, and to their subtending branches (Fig. 2). The vulnerability

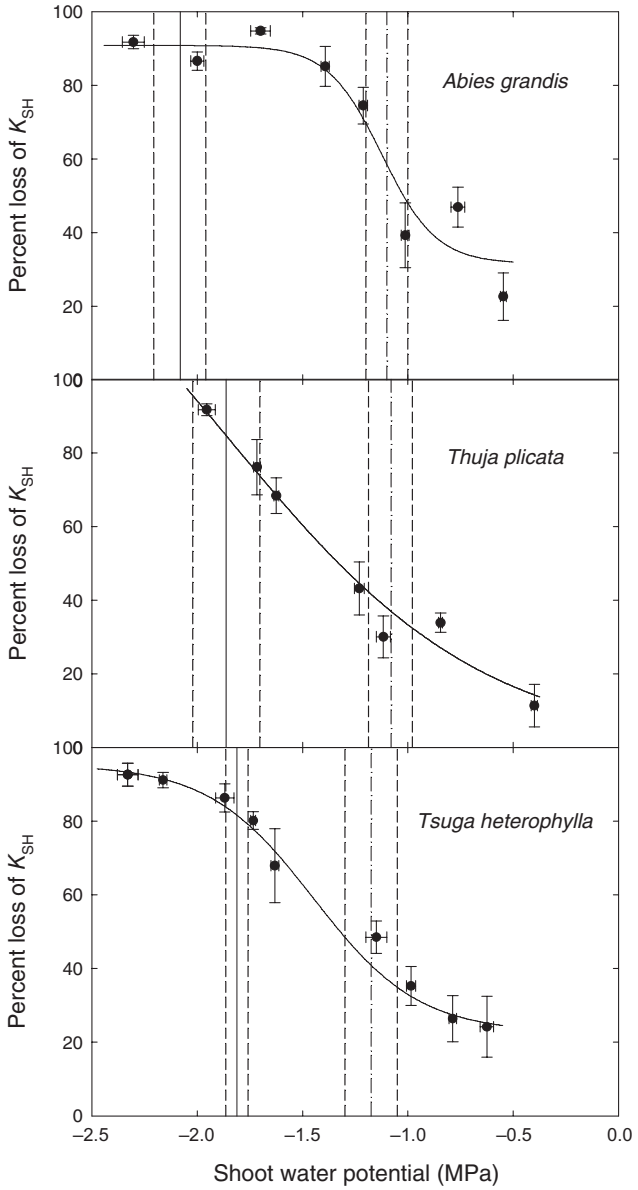

Figure 1. Vulnerability curves for needle-bearing shoots of three co-occurring conifer species. Vertical dash-dotted and solid lines show minimum predawn and midday water potentials, respectively, measured during the growing season. Data are binned by water potential to simplify the figure, but curves were fit using all data. Short-dashed lines indicate standard deviations around the mean water potential values.

curves of both the small- and large-diameter branches were similar both within and among species (Fig. 2). Only *Abies* and *Tsuga* had P_{50} values that differed between the two ranks and in both species the small diameter branches were more resistant to embolism than the large diameter branches (Table 2). Values of P_{12} did not differ between these ranks for any species. Among species, the small diameter branches of *Thuja* had less negative P_{50} values than all other species, and the large branches of *Pseudotsuga* exhibited more negative P_{50} values than all other species. The trunk wood of all species was extremely vulnerable to embolism (Fig. 2). The 95% confidence intervals of the P_{50} values of trunks did not overlap for any species and species ranked from most to least vulnerable were *Tsuga*, *Thuja*, *Abies* and *Pseudotsuga*, respectively.

Predawn (Fig. 1; from McCulloh *et al*. 2011) and midday water potentials (Figs 1 & 2) imply that the vast majority of hydraulic conductance was lost by midday in shoots, but essentially all hydraulic conductivity remained in small diameter branches and trunks. This result was also supported by a comparison of the safety margins (midday water potential – P_{50}) between the three ranks (Fig. 3). The safety margins for all shoots were negative, and ranged from –0.5 MPa to –1.3 MPa in *Tsuga* and *Psuedotsuga*, respectively. In contrast, the much greater resistance to embolism in the stems led to large, positive safety margins, which ranged from 3 to 4 MPa in *Thuja* and *Abies*, respectively. Trunk wood was intermediate with safety margins ranging from 0.3 MPa in *Tsuga* to 0.9 MPa in *Psuedotsuga*.

A strong positive relationship was found between the maximum specific conductivity and stem diameter (Fig. 4, *P*-value = 0.0003) on a log–log plot. No differences were found among species in this relationship. This correlation was driven by increases in tracheid diameter, which increased 2.5–3.0-fold from small diameter branches to trunks (Table 1). Although this relationship is strongly supported by the measurements on the three ranks examined here, the true, biological relationship may more likely be an asymptotic one that levels off at stem diameters between the trunk and large diameter stems, because the tracheid diameter tends to stop increasing basally below the base of the live crown (Dunham *et al*. 2007).

The water release curves indicated capacitance values increased basally (Fig. 5). In a comparison of the regression slopes of the initial, nearly linear portion of the water release curves, which were used to calculate *C* values, all ranks (i.e. small-diameter branches versus large diameter branches versus trunks) were different in *Abies*. In *Thuja*, values in the large branches and trunks were not different, and in *Tsuga* and *Psuedotsuga*, values in the small versus large branches were not different. Nevertheless, all four species exhibited a consistent trend of decreasing *C* as stem diameters narrowed.

Capacitance values were highly correlated with vulnerability curve parameters (Fig. 6, *P*-values for each relationship < 0.001). Within species regressions were not different from pooled data, and the slopes did not differ between P_{12} and P_{50} versus *C* (*P*-value < 0.001). Capacitance was also highly correlated with wood density (Fig. 7, *P*-values < 0.001). Organs with denser wood had lower values of capacitance and the wood density increased from the trunk to the twigs. All species exhibited increases in capacitance with latewood proportions, except *Pseudotsuga*, which had indistinguishable latewood proportion values in the small and large diameter stems. When all stems among all species were compared, a positive relationship was found between the fraction of latewood in annual rings and capacitance (Fig. 8).

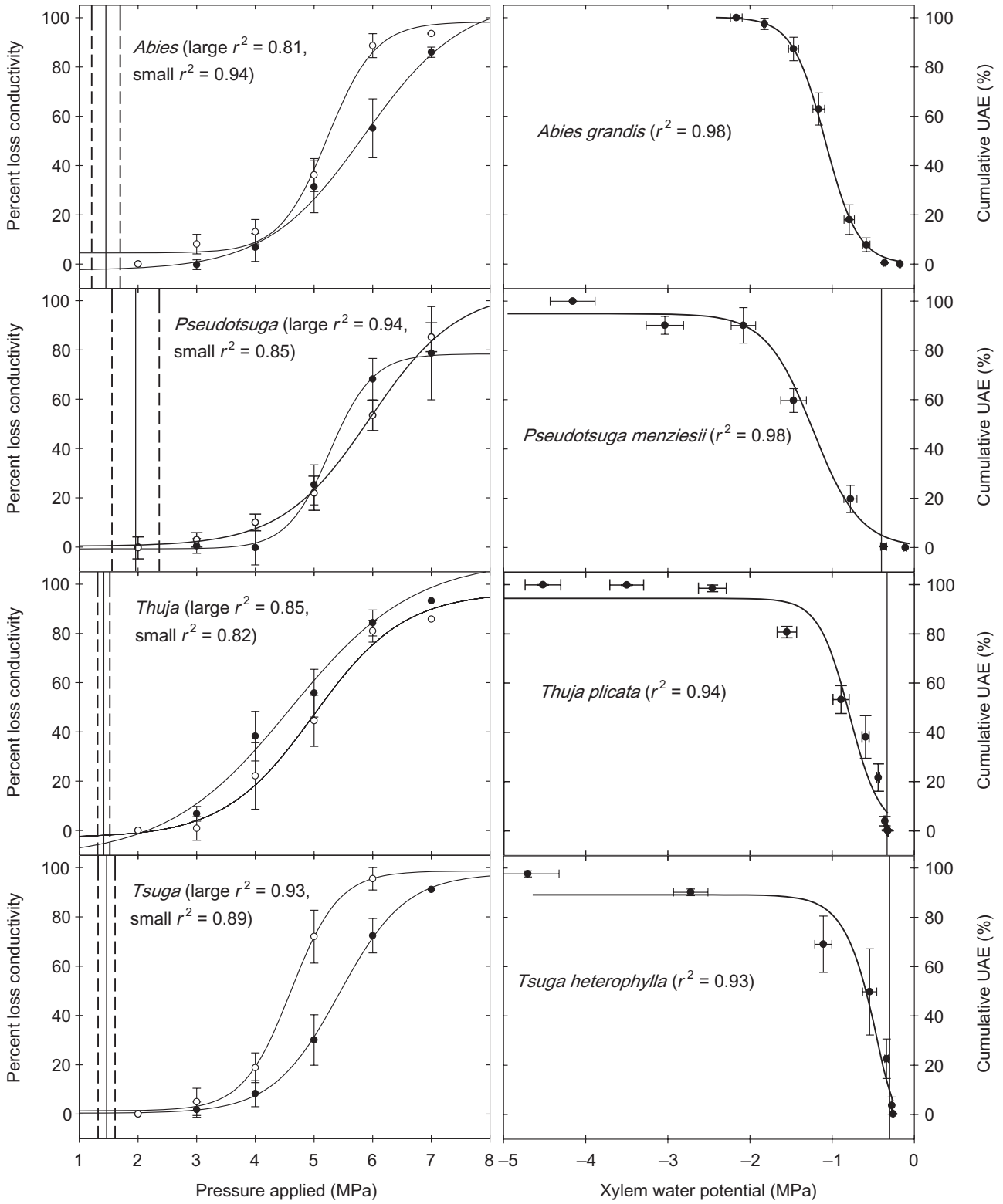

Figure 2. Vulnerability curves for branches (left panels) and trunks (right panels) of four co-occurring conifer species. Branch curves were made for small diameter (closed symbols) and large diameter (open symbols) stems using the air-injection method, and the *x*-axis shows the pressure applied to the stems that induced the loss of conductivity. Vertical lines show seasonal minimum midday water potentials for small diameter branches in the left panels and estimated minimum midday water potentials for trunks in the right panels (see text). Cumulative ultrasonic acoustic emissions were recorded from cores taken from trunks. Data are binned by water potential to simplify the figure, but curves were fitted using all data. We were unable to estimate water potential values for trunk wood of *Abies grandis*. Short-dashed lines indicate standard deviations around the measured midday values in the branches.

Table 2. Maximum specific hydraulic conductivity (k_s) of stems and P_{50} and P_{12} values for stems and shoots

Species	Max k_S – small	Max k_S – large	Max k_S – trunk	P_{50} – small	P_{12} – small	P_{50} – large	P_{12} – large	P_{50} – trunk	P_{12} – trunk	P_{50} – shoots	P_{12} – shoots
Abies grandis	0.24 (0.07)	0.50 (0.06)	4.7 (0.3)	–5.8 (–5.5, –6.1)	–4.3 (–3.6, –4.9)	–5.2 (–5, –5.4)	–4.1 (–3.7, –4.5)	–1.1 (–1.1, –1)	–0.7 (–0.8, –0.6)	–1.0 (–1.1, –0.9)	–0.9 (–0.9, –0.8)
Pseudotsuga menziesii	0.19 (0.03)	0.34 (0.08)	3.4 (0.1)	–5.5 (–5.2, –5.9)	–4.7 (–4.2, –5)	–5.9 (–5.7, –6.1)	–4.4 (–4.0, –4.8)	–1.3 (–1.4, –1.2)	–0.7 (–0.8, –0.5)	–1.2	–0.8
Thuja plicata	0.35 (0.02)	0.65 (0.12)	4.3 (0.3)	–4.6 (–4.3, –5)	–3.1 (–2.3, –3.7)	–5.1 (–4.8, –5.5)	–3.0 (–2.1, –3.4)	–0.8 (–0.9, –0.7)	–0.4 (–0.5, –0.3)	–1.3 (–1.4, –1.2)	–0.9 (–1.0, –0.7)
Tsuga heterophylla	0.34 (0.03)	0.45 (0.07)	3.8 (0.3)	–5.4 (–5.2, –5.7)	–4.3 (–3.9, –4.6)	–4.6 (–4.4, –4.8)	–3.7 (–3.3, –4.1)	–0.6 (–0.7, –0.5)	–0.3 (–0.4, –0.3)	–1.3 (–1.5, –1.1)	–1.0 (–1.3, –0.8)

For k_s values, numbers in parentheses indicate standard errors. For P_{12} and P_{50} values, numbers in parentheses indicate 95% confidence intervals. Vulnerability curve parameters for *Pseudotsuga* shoots are from Woodruff *et al.* (2007) and confidence intervals are not shown. Units used for specific hydraulic conductivity are kg MPa^{-1} m^{-1} s^{-1}, and for P_{12} and P_{50} are MPa.

Figure 3. Safety margins of needle-bearing shoots, branches and trunks for four co-occurring conifer species. Safety margins shown here are the midday water potential (the seasonal minima measured during the summer 2009; Ψ) minus the absolute value of the pressure inducing 50% loss of hydraulic conductance for shoots or conductivity for branches (P_{50}). Negative values indicate that midday water potentials were below P_{50} values. Error bars indicate standard deviations.

DISCUSSION

The reliance on structural attributes that enhance absolute resistance to embolism versus the avoidance of high tensions through dynamic functional traits for tolerance of daily cycles of water stress varied greatly among different organs within each species. In contrast, the amount of embolism resistance in a given organ and the pattern of resistance to water stress across organs were very similar in these co-occurring species. For all species, the shoots and trunk wood were extremely vulnerable to embolism (Figs 1 & 2) and the branches were more resistant. The resistance to embolism in the branches, particularly relative to the water potentials the branches experience (Fig. 3), would prevent emboli from propagating

Figure 4. Specific hydraulic conductivity versus stem diameter for four co-occurring conifer species on a log–log plot. Error bars indicate standard deviations.

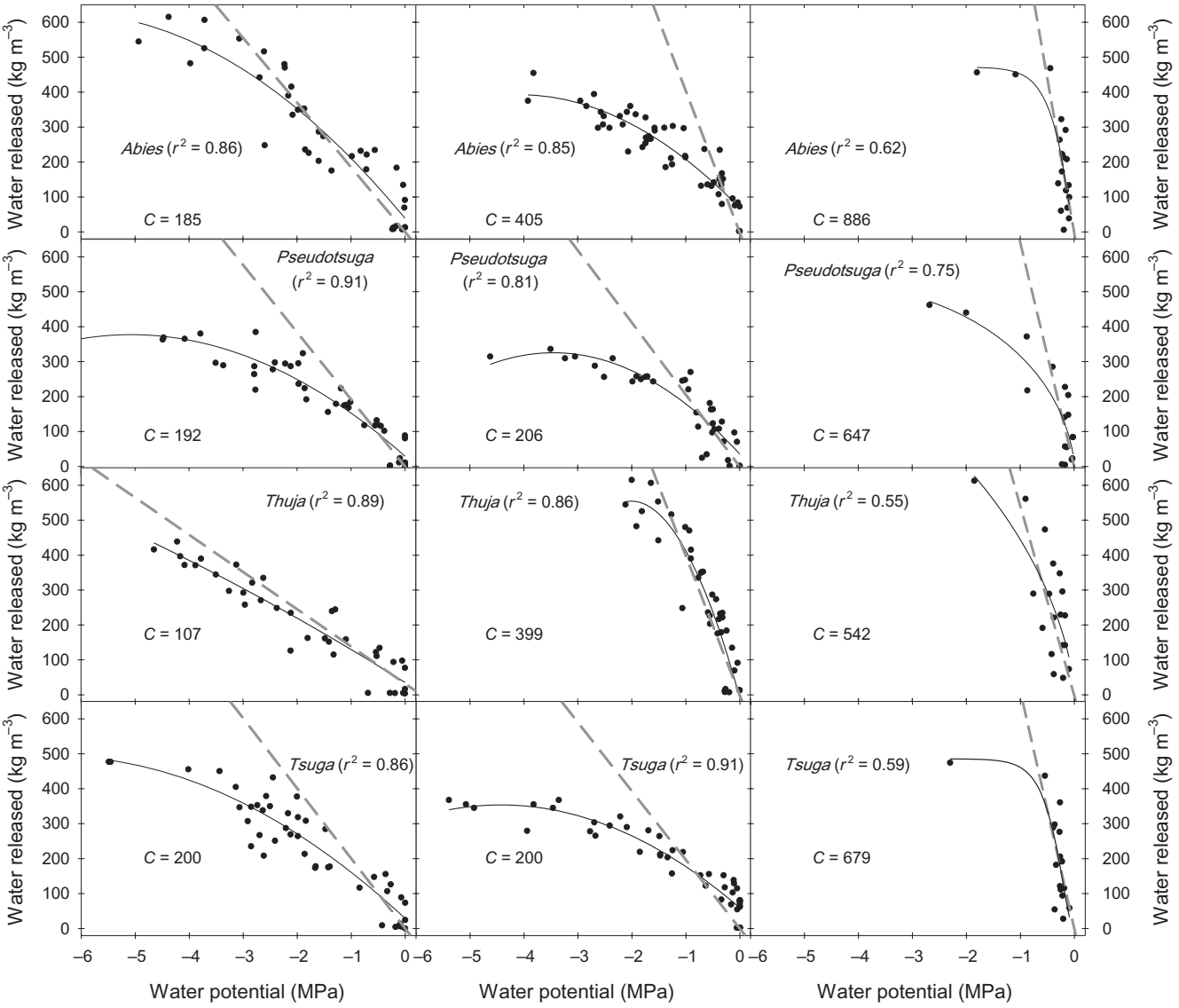

Figure 5. Water release curves for small (left panels) and large (centre panels) diameter branches and trunks (right panels) from four co-occurring conifer species. Solid curves indicate the relationship between the volumetric water released (*y*-axis) and the water potential (*x*-axis). Dashed grey lines were used to calculate the capacitance (C; kg m^{-3} MPa^{-1}) values, which are based on the initial, nearly linear portion of the curve. These lines were forced through the origin for biological accuracy, and the slopes are specified within each panel.

down the branches to the trunk, which would allow the trunk to function as an extremely efficient highway for water transport (Fig. 4). The pattern of increasing capacitance towards the trunks was also remarkably similar among species (Fig. 5), and as the reliance on dynamic buffering of water potentials increased towards the trunks, the P_{50}s and P_{12}s became less negative (Fig. 6), the wood became less dense (Fig. 7) and had a greater proportion of latewood (Fig. 8).

Given the relatively simple structure of conifer wood, how can different organs vary so much in their reliance on structural avoidance of embolism versus reliance on capacitance to buffer water potentials? The source of most capacitive water in conifers seems to be the latewood (Domec & Gartner 2002), which is extremely vulnerable to embolism at low pressures (before the percent loss of conductivity levels off at higher pressures) and essentially may serve much more as a water storage tissue under normal operating pressures than a transport tissue. The inter-tracheid pits are extremely rigid in latewood and may not aspirate when the tracheid embolizes. The vulnerability curves in conifers seem to largely be determined by earlywood resistance to embolism (Domec & Gartner 2002), because of the much greater fraction of the hydraulic conductivity that these larger-diameter tracheids provide. Thus, the proportion of latewood in a wood sample has a large influence on the capacitance of that tissue (Fig. 8). However, the r^2 value (0.65) means that latewood proportion does not entirely determine the amount of water storage. The decline in wood density as stem diameter increases means that larger diameter stems had less cell wall

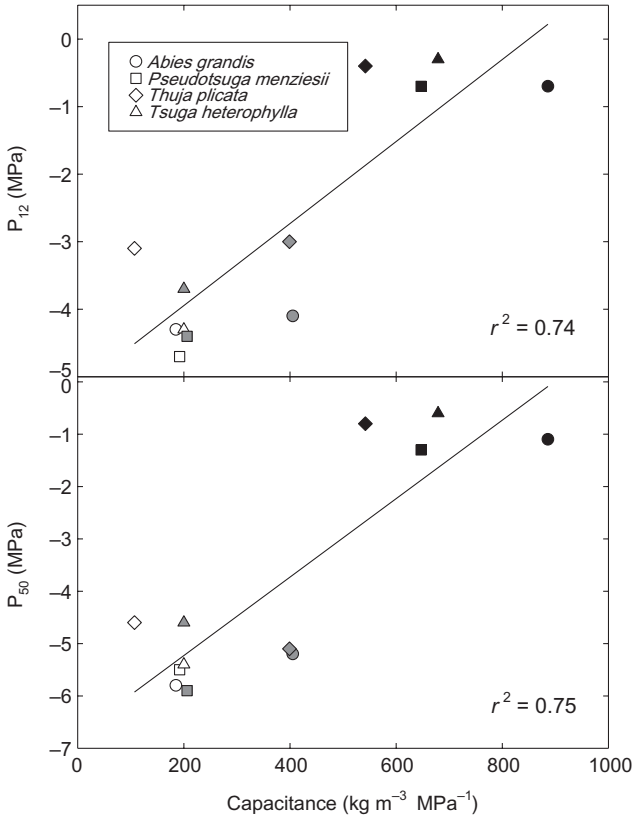

Figure 6. The relationship between vulnerability curve parameters and capacitance in small (open symbols) and large (grey symbols) diameter branches and trunks (closed symbols) in four co-occurring conifer species. P_{12} and P_{50} are the pressures that induce 12% and 50% loss in hydraulic conductivity, respectively. For each line, P-values < 0.01.

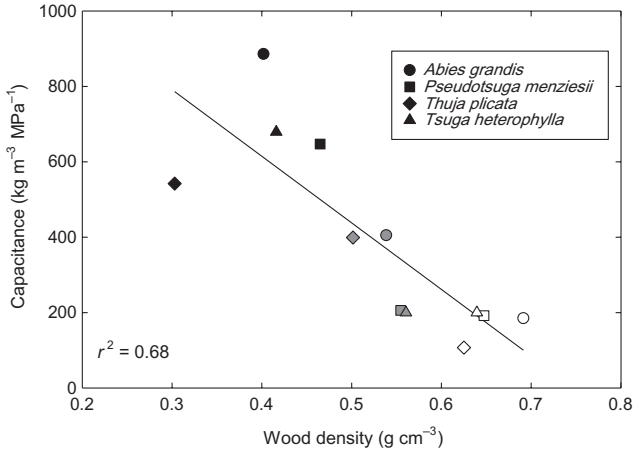

Figure 7. Capacitance versus wood density in small (open symbols) and large (grey symbols) diameter branches and trunks (closed symbols) in four co-occurring conifer species. The P-value = 0.001 for the regression.

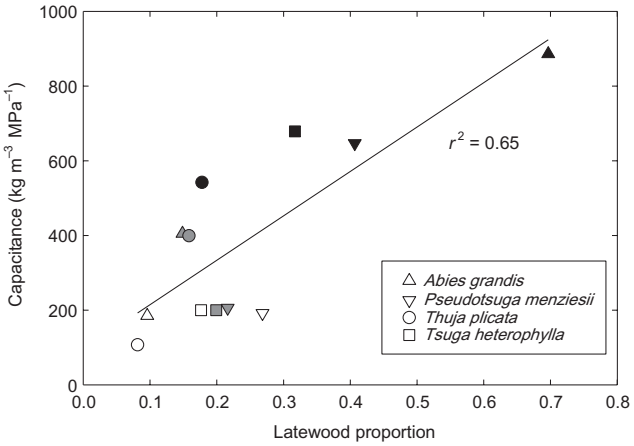

Figure 8. Capacitance versus the proportion of annual rings devoted to latewood in small (open symbols) and large (grey symbols) diameter branches and trunks (closed symbols) in four co-occurring conifer species. The P-value = 0.0016 for the regression.

material per volume than narrower stems, and these intercellular spaces may provide the extra space for stored water.

Despite Zimmermann's (1983) proposal of the idea of hydraulic segmentation decades ago, and its subsequent modification by Tyree and Ewers (1991), we still do not have complete datasets on many species. These authors proposed that to protect the basal portions of plants, the more distal parts should be lost first during periods of drought stress either because of the natural decline in water potential distally (Zimmermann 1983) or because the distal parts of plants become more vulnerable (Tyree & Ewers 1991). One reason for the limited data testing these hypotheses is the difficulty of working with large diameter stems. In research sites where disturbing the soils is discouraged or the species diversity makes identifying roots difficult, both of which were problems in this study, it may not be possible to include roots. However, testing these hypotheses does provide valuable insight into the functioning of these trees. Our data do not support Tyree and Ewer's hypothesis of stems becoming more vulnerable distally, but the higher vulnerability of leaves does fit the idea that the tree has a more vulnerable, disposable organ distal to the higher-investment woody portions of the tree. However, in this case the leaves seem to lose hydraulic conductance everyday and recover it, which may be a way of protecting the hydraulic integrity of the subtending stems without having to discard the leaves.

The results in Figs 1 and 3 suggest that the shoots of all four species lose essentially their entire hydraulic conductance by midday. This pattern has been observed before in the shoots or needles of conifer species and some recovery of hydraulic conductance has been measured by late afternoon, and would need to be completed by the next morning in these long-lived needles (Johnson *et al*. 2009). The prediction of embolisms forming at the pressures that the needles experience at midday was confirmed in *Pseudotsuga* using cryo-scanning electron microscopy (cryo-SEM) analyses

(Woodruff *et al*. 2007). In contrast, the branches were predicted to lose essentially no conductivity, and this prediction was supported by measurements that showed very little native embolism throughout most of the summer in a previous study (McCulloh *et al*. 2011).

Although the vulnerability curves for the leaves, branches and trunks were developed with different techniques, it is likely that they are comparable. Previous work in conifers has found high consistency between rehydration kinetics and acoustic emissions in leaves (Johnson *et al*. 2009), and between acoustic emissions and air injection in wood (Cochard 1992; Rosner *et al*. 2006, 2008, 2009; Barnard *et al*. 2011; Mayr & Rosner 2011).

As more research compares safety margins across leaves and branches, a pattern seems to be developing that species with branches that rely more heavily on structural avoidance of embolism tend to have leaves that lose hydraulic function on daily bases (Woodruff *et al*. 2007; Johnson *et al*. 2009, 2011). The leaves in these species essentially act as 'circuit breakers' (Johnson *et al*. 2012) that hydraulically isolate the branches from experiencing water potentials that could result in loss of hydraulic conductivity, and then are reset each night. We hypothesize that branches in species that exhibit these circuit breakers in their leaves will have low values of capacitance, high wood density, low capacity to refill, large safety margins, little or no ionic regulation of hydraulic conductance [because of the lack of hydrogels in the torus-margo pitting of conifers (Zwieniecki *et al*. 2001)], and possibly leaves with lower stomatal sensitivity (Johnson *et al*. 2012; Meinzer & McCulloh 2013). To our knowledge, the Ogasa *et al*. work (2013) provides the first experimental evidence to support the idea that some species have evolved to rely more heavily on structural features to maintain the transpiration stream at the expense of being able to efficiently refill emboli. Obviously, there are exceptions to the entire predicted suite of traits evolving together because it was also predicted that species with branches that rely more heavily on structure to avoid emboli tend to be anisohydric (Meinzer & McCulloh 2013), yet all four of the species examined here are strongly isohydric (Bauerle *et al*. 1999; Warren *et al*. 2003; McCulloh *et al*. 2011). How these traits relate to where other organs, such as the trunk, exist on the structural versus dynamic continuum is currently unknown because measurements on trunks in mature trees are extremely rare. It may be that in most species, mature trunk wood, like that examined here, is much more vulnerable than branches.

In contrast to the vulnerability of the shoots, the trunk wood, which was also extremely vulnerable, was not predicted to undergo daily cycles of loss and recovery of hydraulic conductivity. Instead, this wood is protected from most emboli because it experiences mild operating pressures (Domec & Gartner 2002). The pressures we calculated ranged from –0.3 to –0.4 MPa in *Tsuga* and *Pseudotsuga*, respectively. Domec *et al*. (2009) measured trunk water potentials with stem psychrometers and found safety margins of approximately 1 MPa in *Pseudotsuga* that were much younger and smaller (diameter at breast height = 64 cm). Those trees, which were about half the diameter of the trees we measured, were much more resistant to embolism than we observed, but the safety margins we found were 0.9 MPa, suggesting the safety margins may stay roughly the same in this organ across ontogeny.

In addition to the positional differences that could lead to differences between trunks and branches in biomechanical demands and absolute tensions, there are fundamental anatomical differences that have been characterized in mature conifers between the juvenile wood of branches and the mature wood of trunk sapwood (Dinwoodie 2000; Domec & Gartner 2002; Dunham *et al*. 2007; Domec *et al*. 2009). Juvenile wood, also called corewood, comprises the first 5–15 years of growth from the pith, and after that mature wood, or outerwood, is made (Panshin & de Zeeuw 1980). Thus, juvenile wood accounts for much more of the wood in branches than in mature trunks. Juvenile wood tends to have smaller diameter tracheids (Table 2), be more resistant to embolism (Domec & Gartner 2002; 2003; Domec *et al*. 2005; Rosner *et al*. 2006) and less stiff (Cave 1968; Lachenbruch *et al*. 2011) than mature wood. These differences are thought to be caused by the smaller tracheid dimensions, smaller pit apertures (Domec *et al*. 2006), and higher microfibril angle in the S2 layer (Barnett & Bonham 2004; Lachenbruch *et al*. 2011), which is the thick, middle layer of the secondary wall of tracheids.

The trend of increasing capacitance with stem diameter was also similar among species. A comparable pattern was observed in the positive relationship between the amount of stored water used per day and basal diameter (Scholz *et al*. 2011). It is also noteworthy that the minimum water potentials for the organs were within the initial, nearly linear portion of the water release curves (Fig. 5). This suggests that stomatal regulation maintains water potentials within the portion of the water release curve that results in the most water released per change in water potential in far more basal regions of the plant than just the leaves or small diameter branches. Although the midday water potentials of the large diameter branches were not measured, they would likely fall close to (but slightly less negative than) the small-diameter branches. These water potential estimates for the large-diameter branches also fall within the linear portion of the water release curve for all species except *Psuedotsuga*. Capacitance is measured relatively rarely, but we are beginning to understand how variable it can be, even within species at different sites. For example, Barnard *et al*. (2011) found greater vulnerability to embolism in trunk wood of populations of *Psuedotsuga menziesii* and *Pinus ponderosa* growing in drier climates than those growing in wetter climates. This seemingly contradictory observation made more sense when the capacitance values showed the drier-site populations had more stored water, which suggested they relied less heavily on structural avoidance of embolism and more on dynamic processes like capacitive discharge of water. Similarly, Fig. 6 indicates a tradeoff between resistance to embolism and capacitance in the trees we measured. Those organs that were more resistant to embolism had small values of capacitance and vice versa.

Despite the striking similarities we observed among species, differences do exist in their hydraulic strategies. For example, Meinzer *et al*. (2007) found that *Tsuga* extracted

less water from the soil surrounding its roots than *Pseudotsuga* was able to. Given that both species have essentially the same hydraulic conductivity and capacitance at the ranks we measured, it seems likely that the stomata of *Tsuga* may be more conservative. This trait difference could explain the less negative safety factor in *Tsuga* shoots compared with *Pseudotsuga* (Fig. 3), and the previously observed avoidance of an increase in native embolism that the three other species suffered from during an extreme heat event (McCulloh *et al*. 2011). These differences make *Tsuga* and *Pseudotsuga* interesting candidates in which to compare the efficiency of the refilling process in shoots and branches.

Within species, the differential reliance of the different organs on structural avoidance of embolism versus dynamic buffering of water potentials highlights the importance of measuring parameters on more than just small-diameter segments and extrapolating from that to the entire organism (Meinzer *et al*. 2010). Similarly, the field of plant hydraulics has focused much attention on embolism avoidance and the importance of P_{50} values, while largely ignoring the dynamic influence of capacitance and refilling (although this topic has received much more consideration recently). It is becoming increasingly clear that the xylem is not just the system of 'dead tubes' many of us learned about in school, but an active and responsive tissue we have yet to fully understand.

ACKNOWLEDGMENTS

The authors are extremely grateful to the staff at the Wind River Field Station, particularly Matt Schroeder. We also thank Danielle Marias for help coring trees. KAM is also indebted to Adam Roddy and Tom Kursar for lengthy conversations about psychrometry. This work was supported by NSF grant IBN 09-19871.

REFERENCES

Barnard D.M., Meinzer F.C., Lachenbruch B., McCulloh K.A., Johnson D.M. & Woodruff D.R. (2011) Climate-related trends in sapwood biophysical properties in two conifers: avoidance of hydraulic dysfunction through coordinated adjustments in xylem efficiency, safety and capacitance. *Plant, Cell & Environment* **34,** 643–654.

Barnett J.R. & Bonham V.A. (2004) Cellulose microfibril angle in the cell wall of wood fibres. *Biological Reviews* **79,** 461–472.

Bauerle W.L., Hinckley T.M., Cermak J., Kucera J. & Bible K. (1999) The canopy water relations of old-growth Douglas-fir trees. *Trees* **13,** 211–217.

Begg J.E. & Turner N.C. (1970) Water potential gradients in field tobacco. *Plant Physiology* **46,** 343–346.

Blackman C.J., Brodribb T.J. & Jordon G.J. (2012) Leaf hydraulic vulnerability influences species' bioclimatic limits in a diverse group of woody angiosperms. *Oecologia* **168,** 1–10.

Brodribb T.J. & Holbrook N.M. (2003) Stomatal closure during leaf dehydration, correlation with other leaf physiological traits. *Plant Physiology* **132,** 2166–2173.

Brodribb T.J. & Holbrook N.M. (2004) Diurnal depression of leaf hydraulic conductance in a tropical tree species. *Plant, Cell & Environment* **27,** 820–827.

Brodribb T.J., Holbrook N.M., Edwards E.J. & Gutierrez M.V. (2003) Relations between stomatal closure, leaf turgor and xylem vulnerability in eight tropical dry forest trees. *Plant, Cell & Environment* **26,** 443–450.

Bucci S.J., Scholz F.G., Campanello P.I., Montti L., Jimenez-Castillo M., Rockwell F.A., . . . Goldstein G. (2012) Hydraulic differences along the water transport system of South American *Nothofagus* species: do leaves protect the stem functionality? *Tree Physiology* **32,** 880–893.

Bucci S.J., Scholz F.G., Perschiutta M.L., Arias N.S., Meinzer F.C. & Goldstein G. (2013) The stem xylem of Patagonian shrubs operates far from the point of catastrophic dysfunction and is additionally protected from drought-induced embolism by leaves and roots. *Plant, Cell & Environment* **36,** 2163–2174.

Cave I.D. (1968) The anisotropic elasticity of the plant cell wall. *Wood Science and Technology* **2,** 268–278.

Chen J.-W., Zhang Q., Li X.-S. & Cao K.-F. (2009) Independence of stem and leaf hydraulic traits in six Euphorbiaceae tree species with contrasting leaf phenology. *Planta* **230,** 459–468.

Choat B., Lahr E.C., Melcher P.J., Zwieniecki M.A. & Holbrook N.M. (2005) The spatial pattern of air seeding thresholds in mature sugar maple trees. *Plant, Cell & Environment* **28,** 1082–1089.

Choat B., Cobb A.R. & Jansen S. (2007) Structure and function of bordered pits: new discoveries and impacts on whole-plant hydraulic function. *New Phytologist* **177,** 608–626.

Choat B., Jansen S., Brodribb T.J., Cochard H., Delzon S., Bhaskar R., . . . Zanne A.E. (2012) Global convergence in the vulnerability of forests to drought. *Nature* **491,** 752–755.

Cochard H. (1992) Vulnerability of several conifers to embolism. *Tree Physiology* **11,** 73–83.

Dinwoodie J.M. (2000) *Timber: Its Nature and Behaviour* 2nd edn, E. & F. N. SPON, London.

Domec J.C. & Gartner B.L. (2001) Cavitation and water storage in bole xylem segments of mature and young Douglas-fir trees. *Trees* **15,** 204–214.

Domec J.C. & Gartner B.L. (2002) Age- and position-related changes in hydraulic versus mechanical dysfunction of xylem: inferring the design criteria for Douglas-fir wood structure. *Tree Physiology* **22,** 91–104.

Domec J.-C. & Gartner B.L. (2003) Relationship between growth rates and xylem hydraulic characteristics in young, mature and old-growth ponderosa pine trees. *Plant, Cell & Environment* **26,** 471–483.

Domec J.-C., Pruyn M.L. & Gartner B.L. (2005) Axial and radial profiles in conductivities, water storage and native embolism in trunks of young and old-growth ponderosa pine trees. *Plant, Cell & Environment* **28,** 1103–1113.

Domec J.C., Lachenbruch B. & Meinzer F.C. (2006) Bordered pit structure and function determine spatial patterns of air-seeding thresholds in xylem of Douglas-fir (*Pseudotsuga menziezii*; Pinaceae) trees. *American Journal of Botany* **93,** 1588–1600.

Domec J.C., Lachenbruch B., Meinzer F.C., Woodruff D.R., Warren J.M. & McCulloh K.A. (2008) Maximum height in a conifer is associated with conflicting requirements for xylem design. *Proceedings of the National Academy of Sciences of the United States of America* **105,** 12069–12074.

Domec J.C., Warren J.M., Meinzer F.C. & Lachenbruch B. (2009) Safety factors for xylem failure by implosion and air-seeding within roots, trunks and branches of young and old conifer trees. *IAWA Journal* **30,** 100–120.

Dunham S.M., Lachenbruch B. & Ganio L.M. (2007) Bayesian analysis of Douglas-fir hydraulic architecture at multiple scales. *Trees* **21,** 65–78.

Hacke U., Sperry J.S., Pockman W.T., Davis S.D. & McCulloh K.A. (2001) Trends in wood density and structure are linked to prevention of xylem implosion by negative pressure. *Oecologia* **126,** 457–461.

Hao G., Hoffmann W.A., Scholz F.G., Bucci S.J., Meinzer F.C., Franco A.C., . . . Goldstein G. (2008) Stem and leaf hydraulics of congeneric tree species from adjacent tropical savanna and forest ecosystems. *Oecologia* **155,** 405–415.

James S.A., Clearwater M.J., Meinzer F.C. & Goldstein G. (2002) Heat dissipation sensors of variable length for the measurement of sap flow in trees with deep sapwood. *Tree Physiology* **22,** 277–283.

Johnson D.M., Woodruff D.R., McCulloh K.A. & Meinzer F.C. (2009) Leaf hydraulic conductance, measured *in situ*, declines and recovers daily: leaf hydraulics, water potential and stomatal conductance in four temperate and three tropical tree species. *Tree Physiology* **29,** 879–887.

Johnson D.M., McCulloh K.A., Meinzer F.C., Woodruff D.R. & Eissenstat D.M. (2011) Hydraulic patterns and safety margins, from stem to stomata, in three eastern US tree species. *Tree Physiology* **31,** 659–668.

Johnson D.M., McCulloh K.A., Woodruff D.R. & Meinzer F.C. (2012) Hydraulic safety margins and embolism reversal in stems and leaves: why are conifers and angiosperms so different? *Plant Science* **195,** 48–53.

Lachenbruch B., Moore J.R. & Evans R. (2011) Radial variation in wood structure and function in woody plants, and hypotheses for its occurrence. In *Age- and Size-Related Changes in Tree Structure and Function* (eds F.C. Meinzer, B.D. Lachenbruch & T.E. Awson), pp. 121–164. Springer-Verlag Dordrecht, Heidelberg, London, New York.

McCulloh K.A., Johnson D.M., Meinzer F.C. & Lachenbruch B. (2011) An annual pattern of native embolism in upper branches of four tall conifer species. *American Journal of Botany* **98,** 1007–1015.

Maherali H., Pockman W.T. & Jackson R.B. (2004) Adaptive variation in the vulnerability of woody plants to xylem cavitation. *Ecology* **85,** 2184–2199.

Maherali H., Moura C.F., Caldeira M.C., Willson C.J. & Jackson R.B. (2006) Functional coordination between leaf gas exchange and vulnerability to xylem cavitation in temperate forest trees. *Plant, Cell & Environment* **29,** 571–583.

Martínez-Vilalta J., Prat E., Oliveras I. & Piñol J. (2002) Xylem hydraulic properties of roots and stems of nine Mediterranean woody species. *Oecologia* **133,** 19–29.

Mayr S. & Rosner S. (2011) Cavitation in dehydrating xylem of Picea abies: energy properties of ultrasonic emissions reflect tracheid dimensions. *Tree Physiology* **31,** 59–67.

Meinzer F.C. & McCulloh K.A. (2013) Xylem recovery from drought-induced embolism: where is the hydraulic point of no return? *Tree Physiology* **33,** 331–334.

Meinzer F.C., James S.A., Goldstein G. & Woodruff D.R. (2003) Whole-tree water transport scales with sapwood capacitance in tropical forest canopy trees. *Plant, Cell & Environment* **26,** 1147–1155.

Meinzer F.C., Warren J.M. & Brooks J.R. (2007) Species specific partitioning of soil water resources in an old-growth Douglas fir-western hemlock forest. *Tree Physiology* **27,** 871–880.

Meinzer F.C., Woodruff D.R., Domec J.-C., Goldstein G., Campanello P.I., Gatti M.G. & Villalobos-Vega R. (2008) Coordination of leaf and stem water transport properties in tropical forest trees. *Oecologia* **156,** 31–41.

Meinzer F.C., Johnson D.M., Lachenbruch B., McCulloh K.A. & Woodruff D.R. (2009) Xylem hydraulic safety margins in woody plants: coordination of stomatal control of xylem tension with hydraulic capacitance. *Functional Ecology* **23,** 922–930.

Meinzer F.C., McCulloh K.A., Lachenbruch B., Woodruff D.R. & Johnson D.M. (2010) The blind men and the elephant: the impact of context and scale in evaluating conflicts between plant hydraulic safety and efficiency. *Oecologia* **164,** 287–296.

Nardini A., Lo Gullo M.A. & Salleo S. (2011) Refilling embolized xylem conduits: is it a matter of phloem unloading? *Plant Science* **180,** 604–611.

Ogasa M., Miki N., Murakami Y. & Yoshikawa K. (2013) Recovery performance in xylem hydraulic conductivity is correlated with cavitation resistance for temperate deciduous tree species. *Tree Physiology* **33,** 335–344.

Panshin A.J. & de Zeeuw C. (1980) *Textbook of Wood Technology*. McGraw-Hill, NY, USA.

Pittermann J., Sperry J.S., Wheeler J.K., Hacke U.G. & Sikkema E.H. (2006) Mechanical reinforcement of tracheids compromises the hydraulic efficiency of conifer xylem. *Plant, Cell & Environment* **29,** 618–628.

Pockman W.T. & Sperry J.S. (2000) Vulnerability to cavitation and the distribution of Sonoran Desert vegetation. *American Journal of Botany* **87,** 1287–1299.

Pratt R.B., Jacobsen A.L., Ewers F.W. & Davis S.D. (2007a) Relationships among xylem transport, biomechanics and storage in stems and roots of nine *Rhamnaceae* species of the California chaparral. *New Phytologist* **174,** 787–798.

Pratt R.B., Jacobsen A.L., Golgotiu K.A., Sperry J.S., Ewers F.W. & Davis S.D. (2007b) Life history type and water stress tolerance in nine California chaparral species (Rhamnaceae). *Ecological Monographs* **77,** 239–253.

Rosner S., Klein A., Wimmer R. & Karlsson B. (2006) Extraction of features from ultrasonic acoustic emissions: a tool to assess the hydraulic vulnerability of Norway spruce trunkwood? *New Phytologist* **171,** 105–116.

Rosner S., Klein A., Müller U. & Karlsson B. (2008) Tradeoffs between hydraulic and mechanical stress responses of mature Norway spruce trunk wood. *Tree Physiology* **28,** 1179–1188.

Rosner S., Karlsson B., Konnerth J. & Hansmann C. (2009) Shrinkage processes in standard-size Norway spruce wood specimens with different vulnerability to cavitation. *Tree Physiology* **29,** 1419–1431.

Scholz F.G., Phillips N.G, Bucci S.J., Meinzer F.C. & Goldstein, G. (2011) Hydraulic capacitance: biophysics and functional significance of internal water sources in relation to tree size. In: *Size- and Age-Related Changes in Tree Structure and Function* (eds F.C. Meinzer, B. Lachenbruch & T.E. Dawson). Springer, Dordrecht.

Shaw D.C., Franklin J.F., Bible K., Klopatek J., Freeman E., Greene S. & Parker G.G. (2004) Ecological setting of the wind river old-growth forest. *Ecosystems* **7,** 427–439.

Sperry J.S. & Saliendra N.Z. (1994) Intra- and inter-plant variation in xylem cavitation in *Betula occidentalis*. *Plant, Cell & Environment* **16,** 279–287.

Tyree M. & Ewers F. (1991) The hydraulic architecture of trees and other woody plants. *New Phytologist* **119,** 345–360.

Tyree M.T. & Hammel H.T. (1972) The measurement of the turgor pressure and the water relations of plants by the pressure-bomb technique. *Journal of Experimental Botany* **23,** 267–282.

Tyree M.T. & Sperry J.S. (1988) Do woody plants operate near the point of catastrophic xylem dysfunction caused by dynamic water stress? *Plant Physiology* **88,** 574–580.

Urli M., Porte A.J., Cochard H., Guengant Y., Burlett R. & Delzon S. (2013) Xylem embolism threshold for catastrophic hydraulic failure in angiosperm trees. *Tree Physiology* **33,** 672–683.

Vilagrosa A., Bellot J., Vallejo V.R. & Gil-Pelegrín E. (2003) Cavitation, stomatal conductance, and leaf dieback in seedlings of two co-occurring Mediterranean shrubs during an intense drought. *Journal of Experimental Botany* **54,** 2015–2024.

Warren C.R., Livingston N.J. & Turpin D.H. (2003) Responses of gas exchange to reversible changes in whole-plant transpiration in two conifer species. *Tree Physiology* **23,** 793–803.

Warton D.I., Wright I.J., Falster D. & Westoby M. (2006) Bivariate line-fitting methods for allometry. *Biological Reviews* **81,** 259–291.

Willson C.J., Manos P.S. & Jackson R.B. (2008) Hydraulic traits are influenced by phylogenetic history in the drought-resistant, invasive genus *Juniperus* (Cupressaceae). *American Journal of Botany* **95,** 299–314.

Woodruff D.R., McCulloh K.A., Warren J.M., Meinzer F.C. & Lachenbruch B. (2007) Impacts of tree height on leaf hydraulic architecture and stomatal control in Douglas-fir. *Plant, Cell & Environment* **30,** 559–569.

Zimmermann M.H. (1978) Hydraulic architecture of some diffuse-porous trees. *Canadian Journal of Botany* **56,** 2286–2295.

Zimmermann M.H. (1983) *Xylem Structure and the Ascent of Sap*. Springer-Verlag, New York, NY, USA.

Zufferey V., Cochard H., Ameglio T., Spring J.-L. & Viret O. (2011) Diurnal cycles of embolism repair and formation in petioles of grapevine (*Vitis vinifera* cv. Chasselas). *Journal of Experimental Botany* **62,** 3885–3894.

Zwieniecki M.A. & Holbrook N.M. (2009) Confronting Maxwell's demon: biophysics of xylem embolism repair. *Trends Plant Science* **14,** 530–534.

Zwieniecki M.A., Melcher P.J. & Holbrook N.M. (2001) Hydrogel control of xylem hydraulic resistance in plants. *Science* **291,** 1059–1062.

Received 1 July 2013; received in revised form 10 October 2013; accepted for publication 21 October 2013

SUPPORTING INFORMATION

Additional Supporting Information may be found in the online version of this article at the publisher's web-site:

Figure S1. Diagram of how segments were cut to measure hydraulic conductivity in trunk wood. Potential cover photo: A misty dawn settles over the tops of trees growing in an old-growth western hemlock-Douglas-fir forest at the Wind River Experimental Field Station.